PAPER *Special Section on Ambient Intelligence and Sensor Networks*

Implementation and Feasibility Study of Co-channel Operation System of Microwave Power Transmissions to IEEE 802.11-Based Batteryless Sensor*

Shota YAMASHITA[†a)], **Norikatsu IMOTO**[†], ***Student Members***, **Takuya ICHIHARA**[††], ***Nonmember***, **Koji YAMAMOTO**[†], ***Senior Member***, **Takayuki NISHIO**[†], ***Member***, **Masahiro MORIKURA**[†], ***Fellow***, ***and*** **Naoki SHINOHARA**[††], ***Member***

SUMMARY In this paper, we study the feasibility of a batteryless wireless sensor supplied with energy by using microwave power transmission (MPT). If we perform co-channel operation of MPT and wireless local area networks (WLANs) for the sake of spectral efficiency, a time division method for MPT and WLAN communications is required to avoid serious interference from MPT to WLAN data transmissions. In addition, to reduce the power consumption of a sensor, the use of power-save operation of the sensor is desirable. We proposed a scheduling scheme that allocates time for MPT and WLAN communications. Specifically, in the proposed scheduling system, an energy source transmits microwave power to a sensor station except when the sensor station transmits data frames or receives beacon frames. In addition, in the proposed scheduling system, we force the remaining energy of the sensor station to converge to a maximum value by adjusting the time interval of data transmission from the sensor station such that the power consumption of the sensor station is reduced. On the basis of the proposition, we implemented a scheduling system and then confirmed that it performed successfully in the conducted experiments. Finally, we discussed the feasibility of the proposed scheduling scheme by evaluating the coverage and then showed that the scheduling scheme can be applied to closed space or room.
key words: *microwave power transmission, IEEE 802.11g-based wireless LAN, co-channel operation, batteryless, time scheduling, sleep mode*

1. Introduction

Wireless sensor networks (WSNs) are a promising technology that will improve our lives in the future [1]. By way of example, medical care systems and disaster alarm systems are WSNs [2], [3]. In these systems, we utilize many wireless sensors and collect sensing data from these sensors through a wireless communication network.

Wireless sensors used in WSNs should be operated without batteries. This is because if stations operate on batteries, it is costly to replace the batteries when sensors are used in difficult places to reach or many sensors are used.

To realize batteryless operation in wireless sensors, we examine the problem using microwave power transmission (MPT) [4]. The reason we use MPT is as follows. There are two technologies that enable batteryless operation. One technology is energy harvesting, for which electronic devices such as solar cells and piezoelectric devices are used. The other technology is wireless power transmission, which utilizes electric resonance, electromagnetic induction, and other components. MPT is one type of wireless power transmission technology, and electric power is transmitted through microwaves. MPT enables us to transmit microwave power far away compared with other wireless power transmission methods. In addition, energy that is obtained by using energy harvesting depends on the ambient environment. On the other hand, we can arbitrarily transmit power anytime if MPT is used.

There are many studies on batteryless wireless sensors and MPT. In [5], [6], energy management requirements for batteryless wireless sensors are described. In [5], adaptive sleep control by using historical data to achieve a long lifetime was proposed. In [6], the necessity of power management for sensors in a WSN was discussed. In [7], the authors conducted experiments related to transmitting microwave power to ZigBee devices and succeeded in both powering the devices and wireless communications. In [4], [8], the authors investigated the use of MPT for powering multiple stations. In [4], the authors conducted experiments in which microwave power was transmitted to several stations with time sharing using a phased array antenna. In contrast, in [8], the authors conducted experiments in which microwave power was transmitted to all stations simultaneously using multiple antennas for MPT while reducing the impact of standing waves caused by multiple reflections and interference.

In this paper, we investigate the application of MPT to an IEEE 802.11g-based wireless sensor. Note that our big goal is to transmit microwave power to IEEE 802.11ah-based wireless sensors [9] in co-channel operation. IEEE 802.11ah-based wireless sensors operate on 900-MHz bands, whereas IEEE 802.11g-based wireless sensors operate on 2.4-GHz bands. However, there are no devices that communicate over IEEE 802.11ah-based WLANs at present because IEEE 802.11ah is in the standardization phase. Therefore, we consider the use of an IEEE 802.11g-based wireless sensor instead of an IEEE 802.11ah-based wireless sensor because IEEE 802.11ah employs the

Manuscript received January 7, 2014.
Manuscript revised April 22, 2014.
[†]The authors are with the Graduate School of Informatics, Kyoto University, Kyoto-shi, 606-8501 Japan.
[††]The authors are with the Research Institute for Sustainable Humanosphere, Kyoto University, Uji-shi, 611-0011 Japan.
*This paper was presented in part at IEEE APCC 2013.
a) E-mail: info14@imc.cce.i.kyoto-u.ac.jp
DOI: 10.1587/transcom.E97.B.1843

same carrier sense multiple access with collision avoidance (CSMA/CA) protocol as IEEE 802.11g.

In a previous study [10], the authors conducted experiments in which an energy source (ES) transmitted microwave power to a sensor station (SS) that communicated over an IEEE 802.11g-based WLAN. From the results of the experiments, two requirements for coexistence of MPT and IEEE 802.11g-based communication were mentioned as follows. First, MPT and wireless communication should not be performed simultaneously. Even when the authors performed adjacent channel operation of MPT and WLAN communications, an SS could not transmit data frames when an ES transmitted microwave power because the SS detected transmitted microwave power on the basis of the CSMA/CA protocol. Thus, the authors suggested that the SS should share the timing information of MPT with the ES and attempt to transmit data frames except when the ES transmits microwave power. Second, the ES must stop transmitting microwave power to the SS when an access point (AP) broadcasts beacon frames. Otherwise, even when microwave power was intermittently transmitted, disassociation from the AP could happen because of the association scheme of the WLAN protocol, or throughput degradation could happen because of the automatic rate selection scheme of the WLAN protocol.

In this paper, to avoid the influence of MPT on WLAN data communications, we set two goals. The first goal is to design a scheduling scheme to solve throughput degradation and disassociation problems caused by the WLAN protocol. The second goal is to confirm the feasibility of the scheduling scheme.

To accomplish these goals, we perform the following steps. First, on the premise of co-channel operation of MPT and IEEE 802.11g-based communications, we propose a scheduling scheme that allocates time for MPT and IEEE 802.11g-based WLAN communications. By performing co-channel operation of MPT and WLAN communications, we are also able to achieve high spectral efficiency, i.e., a dedicated frequency band for MPT is not required. In addition, considering that the supplied power to the SS for MPT is very small (on the order of milliwatts) in general, we attempt a method that lets the ES transmit microwave power as long as possible, whereas the SS uses power-save operation to reduce its consumed power; thus, the duration of each MPT is set to be longer than that of each data transmission. Then, on the basis of this proposed scheme, we implement a system and conduct experiments to confirm the expected performance. For the feasibility study, we assume that the remaining energy of the SS certainly increases when the ES transmits microwave power. In addition, radio radiation protection guidelines related to microwave effects on humans accordingly limit the equivalent isotropically radiated power (EIRP) of MPT [11]. Thus, in the experiments, we use a large horn antenna for MPT because antenna size is irrelevant to accomplish the goals of this paper. Finally, we discuss the feasibility of the system using our proposed scheduling scheme. Specifically, we estimate the maximum allowable distance at which the SS obtains sufficient power to perform wireless communication such that the radio radiation protection guidelines are satisfied. In addition, we also discuss the feasibility of the case where microwave power is transmitted to an IEEE 802.11ah-based wireless sensor using our proposed scheme in co-channel operation. From these results, we can determine what application our proposed scheme can be utilized for in terms of the distance at which the SS obtains sufficient power.

We would like to emphasize that the motivation of this paper is to solve throughput degradation and disassociation problems caused by the WLAN protocol. To solve these problems, we design a scheduling scheme only for a single SS because these problems can happen even when microwave power is transmitted to a single SS. Thus, MPT for multiple stations and directivity control for a transmission antenna are out of the scope of this paper. Note that in [4], [8], the authors discussed how to transmit microwave power toward multiple stations.

This paper is organized as follows. In Sect. 2, we show the setup of the experiment. In Sect. 3, we describe the power-saving operation of a WLAN module. In Sect. 4, we propose the scheduling scheme. In Sect. 5, we describe the experiments and the results. Then, we discuss the feasibility of the proposed scheduling scheme using a link budget in Sect. 6. Finally, we conclude this paper in Sect. 7.

2. Setup of Experiment

Figure 1 shows the setup of the experiment. In this experiment, there are three devices: an ES, AP, and SS.

We explain the whole process of operation. First, the SS measures its remaining energy and then calculates the timing of the next data transmission using the history of the remaining energy. Next, the SS transmits a data frame including the timing of the next data transmission to the ES through the AP. On the basis of the timing of the next data transmission of the SS, the ES transmits microwave power toward the SS, and the remaining energy of the SS increases.

We explain the details of each device. The ES consists of a horn antenna, an amplifier, a radio frequency signal generator, a microcontroller board, a laptop, and a WLAN module. The microcontroller board determines whether microwave power is transmitted. The microcontroller board also forwards data frames to the laptop, and then the laptop displays the transmission data from the SS. Note that the laptop only displays these data for analysis, not for control of the MPT.

The SS consists of a rectenna (a patch antenna and a rectifier), a capacitor, a DC-DC converter, a microcontroller board, a sensing device, and a WLAN module. The SS is powered by microwave power transmitted from the ES, obtains sensing data, and transmits data frames to the ES. The microcontroller board and the WLAN module of the SS are powered by the capacitor. The microcontroller board determines the power-save operation of the WLAN module and then makes the WLAN module operate in sleep mode except

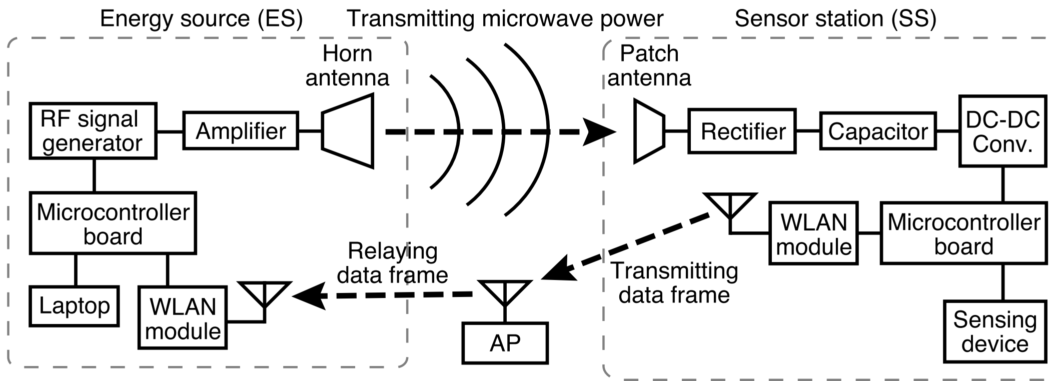

Fig. 1 Experimental setup.

when the SS transmits data frames. Before the SS transmits data frames, the microcontroller board measures a physical quantity with the use of the sensing device and calculates the remaining energy stored in the capacitor by measuring the capacitor voltage. Note that the specific contents of the sensing data are out of the scope of this paper, and we treat the remaining energy stored in the capacitor of the SS as sensing data. From the history of the remaining energy, the SS estimates the supplied power when the ES transmits microwave power. Note that in this experiment the supplied power is almost constant when the ES transmits microwave power. Then, the microcontroller board determines the timing of the next data transmission. The microcontroller board generates a data frame containing both the sensing data and the information of the timing of the next data transmission, and the SS transmits the data frame to the ES through the AP. When the ES transmits microwaves, the rectenna receives and rectifies the microwaves, charging the capacitor.

The AP periodically broadcasts beacon frames to manage the network. When the AP receives a data frame from the SS, it forwards the data frame to the ES.

3. Power-Save Operation of WLAN Module

The primary component of the total power consumption of the SS is the power consumption of the WLAN module. Thus, to save energy, the SS is required to use a power-save operation of the WLAN module, except when the SS communicates. Note that if we do not use the power-save operation, the energy that the SS consumes increases and would be significantly more than the supplied energy from MPT. In this section, we introduce the power-save operation of the WLAN module.

Figure 2 shows the relationship among the timing when the AP broadcasts beacon frames, the state of the power consumption of the SS, and the mode of the power-save operation of the WLAN module. Note that the pattern of power consumption was obtained from a preliminary experiment, and the details are discussed in Sect. 5.

As shown in Fig. 2, the AP periodically broadcasts beacon frames. In addition, beacon frames that contain delivery traffic indication map (DTIM) information are broadcasted

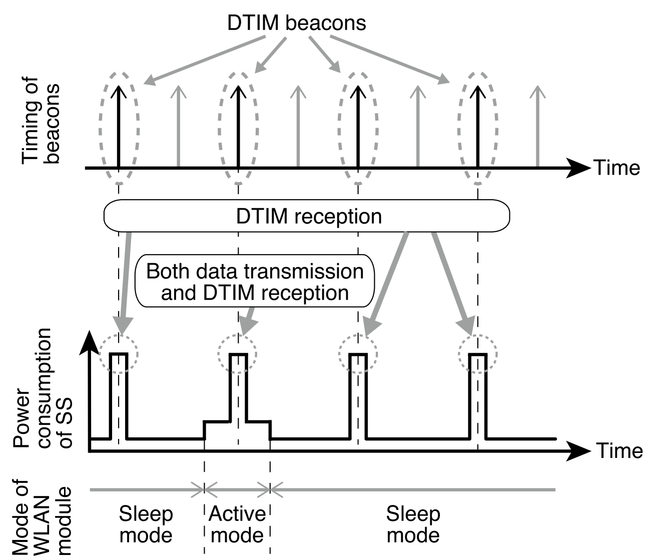

Fig. 2 Power consumption of SS during communication.

every predetermined number of beacon frames. Hereafter, the beacon frames that contain DTIM information are simply referred to as "DTIM beacons."

There are two modes related to the power-save operation of the WLAN module: active and sleep modes. The microcontroller board switches these two modes of the WLAN module depending on the demand for transmission. As shown in Fig. 2, the power consumption of the SS is large when the SS transmits data frames or receives DTIM beacons because the WLAN module is completely powered to perform wireless communication.

For the SS to transmit data frames, before the DTIM beacon is broadcasted, the microcontroller board switches the mode of the WLAN module from sleep mode to active mode. In this case, the SS attempts to transmit data frames just before it receives the DTIM beacon. When a certain time has elapsed since the WLAN module is switched to active mode, the microcontroller board switches the mode of WLAN module from active mode to sleep mode. In sleep mode, the SS only receives DTIM beacons to maintain the association with the AP and does not transmit data frames.

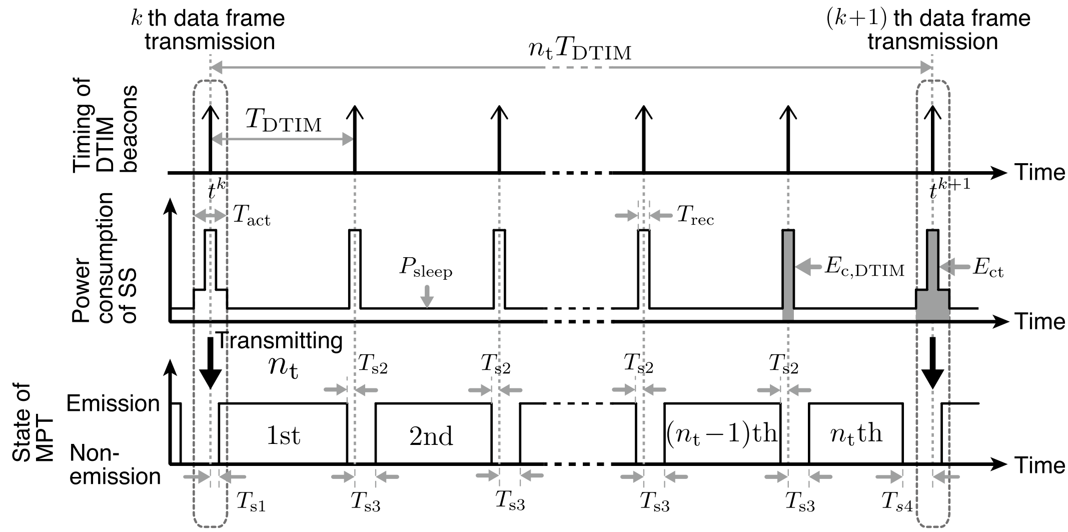

Fig. 3 Operational flow of proposed scheduling system.

4. Proposed Microwave Power and Data Transmission Scheduling

In this section, we explain our proposed scheduling scheme. In this scheduling scheme, an SS that has little remaining energy refrains from data transmission to save energy, i.e., the SS does not transmit data frames periodically.

4.1 Requirements for Microwave Power and Data Transmission

To reduce the power consumption of the SS, it is desirable that the voltage of the capacitor of the SS is as large as the withstand voltage of the capacitor. The reason is as follows. Regarding the efficiency of the DC-DC converter connected after the capacitor, an input voltage that is close to the output constant voltage is desirable. In addition, in this experiment, the withstand voltage of the capacitor is lower than the constant output voltage of the DC-DC converter. Thus, we set the target energy of the capacitor at the energy stored in the capacitor charged up to the withstand voltage. Hereinafter, this energy is referred to as $E_{\max}$.

As clarified in [10], the SS should share the information on the timing of MPT such that the SS transmits data frames when the ES does not transmit microwave power. In addition, as also clarified in [10], the ES should stop MPT around the timing of DTIM beacons because if the ES transmits microwave power around the timing of DTIM beacons, the SS is disassociated from the AP.

4.2 Operational Flow

Figure 3 shows the operational flow of the proposed scheduling scheme. This figure shows the relationship among the timing when the AP broadcasts DTIM beacons, the state of the power consumption of the SS, and the state of MPT.

Table 1 Definitions of parameters.

Symbols	Definitions
$E_{\max}$	Maximum allowable energy that capacitor stores
$T_{\rm DTIM}$	DTIM interval
$T_{\rm s1}$	Guard time between DTIM beacon and MPT when transmitting data
$T_{\rm s2}$	Guard time between MPT and DTIM beacon when in sleep mode
$T_{\rm s3}$	Guard time between DTIM beacon and MPT when in sleep mode
$T_{\rm s4}$	Guard time between MPT and DTIM beacon when transmitting data

Table 2 Definitions of predetermined constants.

Symbols	Definitions
$E_{\rm ct}$	Energy consumption of SS for data frame transmission
$E_{\rm c,DTIM}$	Energy consumption of SS for DTIM reception
$P_{\rm sleep}$	Power consumption of SS in sleep mode
$T_{\rm act}$	Duration of active mode of SS
$T_{\rm rec}$	Duration of SS energy consumption to receive DTIM beacon

The parameters and constants used in Fig. 3 are summarized in Tables 1 and 2, respectively. Note that the constants shown in Table 2 are predetermined from measurements of the power consumption of the SS using a DC power source.

4.3 Sharing Information on Timing of Next Data Transmission

The SS, just before a data transmission, determines the timing of the next data transmission on the basis of the remaining energy of the SS so as to maintain its energy close to $E_{\max}$. Then, the SS informs the ES of the timing of the next data transmission, i.e., the timing of the active mode. In addition, the SS also informs the ES whether the SS requires MPT.

We explain the details of sharing the information below. Let t_k denote the timing of the kth data frame transmission of the SS. As explained in Sect. 3, because the SS transmits data frames immediately before the SS receives DTIM beacons, t_{k+1} is given by $t_{k+1} = t_k + n_t T_{\mathrm{DTIM}}$ ($n_t = 1, 2, \ldots$), where T_{DTIM} represents the DTIM interval. The data frame consists of sensing data and n_t. On the basis of the informed n_t from the SS, the ES calculates t_{k+1}. Then, the ES transmits microwave power in $[t_k, t_{k+1}]$, except during the transmission of the DTIM beacons, as shown in Fig. 3 such that the microwave power does not prevent the SS from the reception of DTIM beacons.

To inform the ES of not only the timing of the next active mode but also the information regarding whether the SS requires MPT, we introduce an optional value where $n_t = 0$, whereas the ES always transmits microwave power when $n_t = 1, 2, \ldots$. When $n_t = 0$, t_{k+1} is set as $t_{k+1} = t_k + T_{\mathrm{DTIM}}$, and the ES does not transmit microwave power during $[t_k, t_{k+1}]$.

To summarize, when the SS informs the ES of n_t (= $0, 1, 2, \ldots$) to the ES at t_k, t_{k+1} is given by

$$t_{k+1} = \begin{cases} t_k + T_{\mathrm{DTIM}} & \text{if } n_t = 0 \\ t_k + n_t T_{\mathrm{DTIM}} & \text{if } n_t = 1, 2, \ldots. \end{cases} \quad (1)$$

Recall that by informing the ES of n_t, the ES calculates t_{k+1} and determines whether the ES transmits microwave power.

4.4 Method to Determine Appropriate n_t

We explain the method to determine the appropriate value for n_t such that the energy stored in the capacitor of the SS converges to $E_{\max}$ as explained in Sect. 4.1. Let $n^{\star}_{t,k}$ denote n_t transmitted with the kth data transmission. The value of $n^{\star}_{t,k}$ impacts the energy stored in the capacitor in the $(k+1)$th data transmission.

When the SS is switched from sleep mode to active mode, the SS estimates both the energy consumption of the SS and the supplied energy to the SS. Let the "estimated energy consumption of the SS during $[t_k, t_{k+1}]$" and the "estimated supplied energy to the SS during $[t_k, t_{k+1}]$" to a certain n_t be denoted by $\hat{e}_c(n_t)$ and $\hat{e}_t(n_t)$, respectively. The SS calculates $\hat{e}_c(n_t)$ as

$$\begin{aligned} \hat{e}_c(n_t) &= E_{ct} + P_{\mathrm{sleep}}(T_{\mathrm{DTIM}} - T_{\mathrm{act}}) \\ &\quad + (n_t - 1)[E_{c,\mathrm{DTIM}} + P_{\mathrm{sleep}}(T_{\mathrm{DTIM}} - T_{\mathrm{rec}})]. \end{aligned} \quad (2)$$

Then, we explain how to calculate $\hat{e}_t(n_t)$. First, the SS calculates the aggregated duration during which the ES transmits microwave power in the time interval $[t_k, t_{k+1}]$. Let $t_{tr}(n_t)$ denote the aggregated duration to a certain n_t, and $t_{tr}(n_t)$ is evaluated as

$$t_{tr}(n_t) = \begin{cases} 0 & \text{if } n_t = 0 \\ n_t T_{\mathrm{DTIM}} - (T_{s1} + T_{s4}) & \\ \quad -(n_t - 1)(T_{s2} + T_{s3}) & \text{if } n_t = 1, 2, \ldots. \end{cases} \quad (3)$$

Second, the SS estimates the supplied power to the SS when the ES transmits microwave power. Let $\hat{p}_r$ denote the estimated supplied power when the ES transmits microwave power. Note that the SS measures the energy stored in the capacitor before every data transmission, and let e_k denote the measured energy before the kth data transmission. On the basis of e_{k-1}, e_k, and $n^{\star}_{t,k-1}$, the SS updates $\hat{p}_r$ as

$$\hat{p}_r = \begin{cases} \hat{p}_r & \text{if } n^{\star}_{t,k-1} = 0 \\ \dfrac{e_k - e_{k-1} + \hat{e}_c(n^{\star}_{t,k-1})}{t_{tr}(n^{\star}_{t,k-1})} & \text{if } n^{\star}_{t,k-1} = 1, 2, \ldots. \end{cases} \quad (4)$$

Last, using $t_{tr}(n_t)$ and $\hat{p}_r$, $\hat{e}_t(n_t)$ is evaluated by

$$\hat{e}_t(n_t) = \hat{p}_r t_{tr}(n_t). \quad (5)$$

Using e_k, $\hat{e}_c(n_t)$, and $\hat{e}_t(n_t)$, the SS determines $n^{\star}_{t,k}$. Specifically, the SS determines $n^{\star}_{t,k}$ such that the estimated energy stored in the capacitor of the SS in the $(k + 1)$th data transmission is nearest to $E_{\max}$. Let $\hat{e}_{k+1}(n_t)$ denote the estimated energy in the $(k + 1)$th data transmission to a certain n_t, and $\hat{e}_{k+1}(n_t)$ is estimated by

$$\hat{e}_{k+1}(n_t) = e_k + \hat{e}_t(n_t) - \hat{e}_c(n_t). \quad (6)$$

Using $\hat{e}_{k+1}(n_t)$, the SS determines $n^{\star}_{t,k}$ as

$$n^{\star}_{t,k} = \begin{cases} 0 & \text{if } \hat{e}_{k+1}(n_t) \geq E_{\max}\ , \forall n_t, \\ \displaystyle\arg\min_{n_t \in \mathcal{N}} E_{\max} - \hat{e}_{k+1}(n_t) & \text{otherwise}, \end{cases} \quad (7)$$

where $\mathcal{N} = \{n | \hat{e}_{k+1}(n) < E_{\max}, n = 1, \ldots, N\}$, and N represents the maximum value for $n^{\star}_{t,k}$. In addition, in (7), $n^{\star}_{t,k}$ has a unique value because $E_{\max} - \hat{e}_{k+1}(n_t)$ has different values for n_t.

5. Experiment

5.1 Parameters

Figure 4 shows the position of each device and the distances between antennas. The SS is set in front of the horn antenna of the ES, and both the WLAN module of the ES and the AP are set behind the horn antenna to prevent serious interference. Figure 5 shows the SS and the horn antenna of the ES.

We use "Arduino Fio" [12] as the microcontroller board of the ES and the SS. Moreover, we use "XBee Wi-Fi"

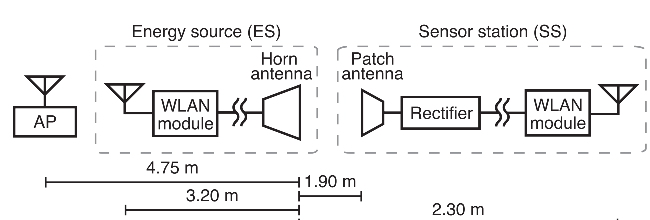

Fig. 4 Position of each device in experimental setup.

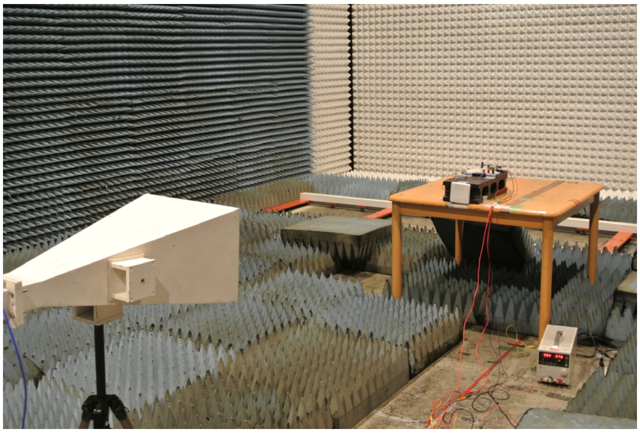

Fig. 5 Experimental setup of horn antenna and SS.

Table 3 Values of parameters.

Parameters	Values
E_{max}	36.45 J
T_{DTIM}	10.24 s
T_{s1}	100 ms
T_{s2}	200 ms
T_{s3}	800 ms
T_{s4}	1000 ms

Table 4 Values of predetermined constants.

Constants	Values
E_{ct}	21.51 mJ
$E_{\mathrm{c,DTIM}}$	17.4 mJ
P_{sleep}	6.6 mW
T_{act}	90 ms
T_{rec}	40 ms

[13] as the WLAN modules of the ES and the SS. The SS, ES, and AP transmit or receive user datagram protocol (UDP) data using 2.446–2.468 GHz bands. On the other hand, the ES transmits microwave power on the frequency of 2.457 GHz. The input power of the horn antenna is 12.8 W when the ES transmits microwave power. The antenna gain of the horn antenna is 19 dBi, and that of the patch antenna is 7.7 dBi. The capacitor of the SS has a capacitance of 10 F and a dielectric strength of 2.7 V. The DC-DC converter of the SS converts the capacitor voltage to 3.3 V, which is required for the input voltage for both the microcontroller board and the WLAN module.

Tables 3 and 4 show the parameters and the constants, respectively. The constants shown in Table 4 are predetermined from the measurement of the consumed power when the SS is powered by using a DC power source.

5.2 Experimental Results

Figure 6 shows the power consumption of the SS and the state of MPT when we operate the implemented system. In Fig. 6, the SS receives DTIM beacons when the power consumption of the SS is high, and the SS operates in sleep mode when the power consumption of the SS is low. As

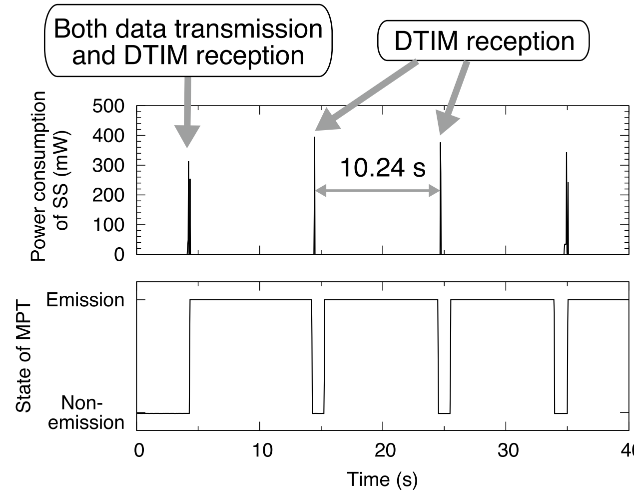

Fig. 6 Operation of our implemented system.

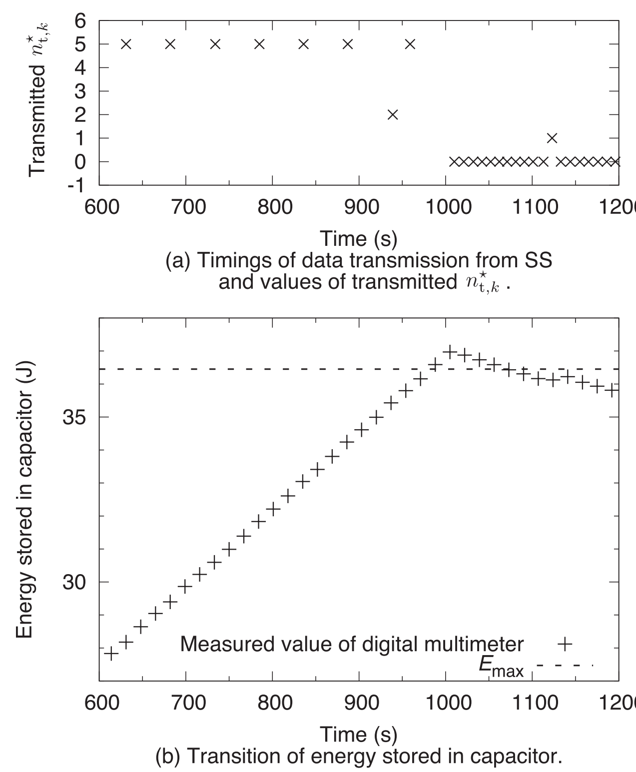

Fig. 7 Energy stored in the capacitor and timing of data transmission.

shown in Fig. 6, the SS receives DTIM beacons when the ES does not transmit microwave power, and the SS operates in sleep mode when the ES transmits microwave power. Thus, we confirmed the successful implementation of the scheduling scheme shown in Fig. 3.

Figure 7(a) shows both the timings of data frame transmissions of the SS and the values of the transmitted $n^{\star}_{t,k}$, and Fig. 7(b) shows the transition of the energy stored in the capacitor of the SS. As shown in Fig. 7(b), the energy stored in the capacitor increased and successfully converged to E_{max}. This occurs because the ES transmits microwave

Table 5 Power density at each antenna when input power of horn antenna is 12.8 W.

Position of antenna	Power density
Patch antenna of SS	19.44 W/m^2
WLAN module antenna of SS	11.72 W/m^2
Antenna of AP	1.67 mW/m^2
WLAN module antenna of ES	26.6 μW/m^2

Table 6 Link budget using experimental results.

	Values
Input power of horn antenna	41.07 dBm
Gain of horn antenna	19 dBi
Free space propagation loss	45.83 dB
Gain of patch antenna	7.7 dBi
Power efficiency of rectifier	−6.01 dB
Estimated output power of rectifier	15.93 dBm
Measured output power of rectifier	15.31 dBm

power in response to the data frames from the SS in our implemented system. In other words, the ES does not transmit microwave power if the SS fails to transmit data frames. In addition, if the SS fails to receive DTIM beacons because of microwaves for MPT, the power consumption of the SS exceeds the supplied power for MPT, and then the energy stored in the capacitor decreases.

In Fig. 7(b), the average increment of the energy stored in the capacitor is 22.9 mW when the energy increases. When both the power consumption of the SS and the duration over which the ES does not transmit microwave power are taken into account, the obtained power of the SS when the ES transmits microwave power is estimated as

$$\frac{22.9\,\mathrm{mW}\cdot T_{\mathrm{DTIM}} + E_{\mathrm{c,DTIM}} + P_{\mathrm{sleep}}(T_{\mathrm{DTIM}} - T_{\mathrm{rec}})}{T_{\mathrm{DTIM}} - (T_{\mathrm{s2}} + T_{\mathrm{s3}})} \approx 34.5\,\mathrm{mW}. \tag{8}$$

Table 5 shows the power density at each antenna when the ES transmits microwave power. Table 6 shows the link budget related to the experimental results. Using the power density at the patch antenna, the gain of the patch antenna, and the measured output power from the rectifier, the power efficiency of the rectifier is calculated.

6. Feasibility of Proposed System

We discuss the feasibility of our proposed system by examining the maximum distance between the ES and the SS.

Regarding that microwaves affect human bodies, there are radio radiation protection guidelines that limit the power density at a certain distance from the power transmitter antenna in Japan [11]. According to these guidelines, the limited maximum power density is 10 W/m^2 if we use 2.4 GHz or 6 W/m^2 if we use 900 MHz. In addition, we regard radio wave propagation as free space propagation.

Figure 8 shows the positions of devices for this analysis, and the definitions of the symbols used in Fig. 8 are summarized in Table 7, where

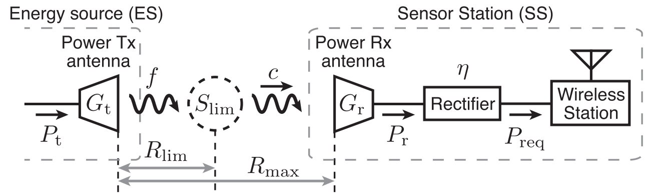

Fig. 8 Positions of devices for analysis.

Table 7 Definitions of symbols used in Fig. 8.

Symbols	Definitions	Units
c	Speed of light	m/s
f	Frequency for MPT	Hz
P_{t}	Input power of power transmitter antenna	W
G_{t}	Gain of power transmitter antenna	
R_{lim}	Maximum allowable distance satisfying guidelines	W
S_{lim}	Power density limit of guidelines	W/m^2
G_{r}	Gain of power receiver antenna	
P_{r}	Output power of power receiver antenna	W
η	Power efficiency of rectifier	
P_{req}	Required supplied power to SS	W
R_{max}	Maximum distance at which system is realized	m

$$S_{\mathrm{lim}} = \frac{G_{\mathrm{t}}P_{\mathrm{t}}}{4\pi R_{\mathrm{lim}}{}^2} \Leftrightarrow G_{\mathrm{t}}P_{\mathrm{t}} = 4\pi S_{\mathrm{lim}} R_{\mathrm{lim}}{}^2. \tag{9}$$

Referring to the Friis transmission formula and using (9), P_{r} is written as

$$P_{\mathrm{r}} = G_{\mathrm{r}}G_{\mathrm{t}}P_{\mathrm{t}}\left(\frac{c}{4\pi R_{\mathrm{max}} f}\right)^2 = \frac{G_{\mathrm{r}}S_{\mathrm{lim}}}{4\pi}\left(\frac{R_{\mathrm{lim}}c}{R_{\mathrm{max}} f}\right)^2. \tag{10}$$

Hence, P_{req} is written as

$$\begin{aligned} P_{\mathrm{req}} &= \eta P_{\mathrm{r}} = \eta G_{\mathrm{r}}G_{\mathrm{t}}P_{\mathrm{t}}\left(\frac{c}{4\pi R_{\mathrm{max}} f}\right)^2 \\ &= \frac{\eta G_{\mathrm{r}}S_{\mathrm{lim}}}{4\pi}\left(\frac{R_{\mathrm{lim}}c}{R_{\mathrm{max}} f}\right)^2. \end{aligned} \tag{11}$$

As shown in (11), P_{req} is independent of G_{t} and P_{t}.

On the basis of the proposed scheduling system described in Sect. 4, we assume that the operational flows related to the SS and the ES are followed in Fig. 9. The definitions of the symbols used in Fig. 9 are summarized in Table 8. Note that duty ratio D is defined as the ratio of the active time of the SS to the cycle time T. We provide equations related to the symbols used in Fig. 9. $\overline{P_{\mathrm{c}}}$ and $\overline{P_{\mathrm{s}}}$ are defined as

$$\begin{aligned} \overline{P_{\mathrm{c}}} &:= [DTP_{\mathrm{com}} + (1-D)TP_{\mathrm{sleep}}]/T \\ &= DP_{\mathrm{com}} + (1-D)P_{\mathrm{sleep}} \end{aligned} \tag{12}$$

and

$$\overline{P_{\mathrm{s}}} := (1-D)TP_{\mathrm{req}}/T = (1-D)P_{\mathrm{req}}, \tag{13}$$

respectively. As shown in (12) and (13), both $\overline{P_{\mathrm{c}}}$ and $\overline{P_{\mathrm{s}}}$ are independent of T. Because the SS receives the minimum power necessary to perform wireless communication,

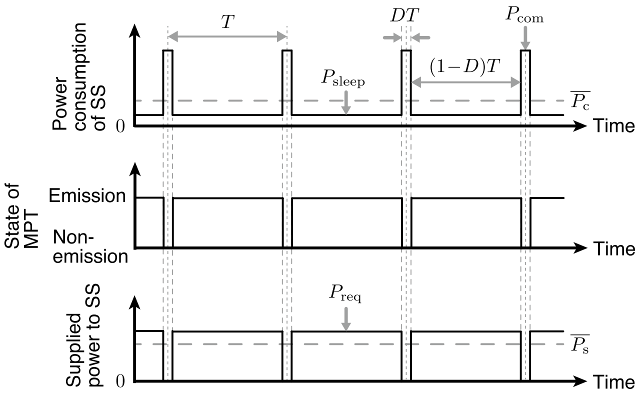

Fig. 9 Assumed operational flow for analysis.

Table 8 Definitions of symbols used in Fig. 9.

Symbols	Definitions	Units
T	Period with which SS communicates	s
D	Duty ratio	
P_{com}	Power consumption of SS to communicate	W
P_{req}	Required supplied power to SS	W
P_{sleep}	Power consumption of SS in sleep mode	W
$\overline{P_{\mathrm{c}}}$	Average power consumption of SS	W
$\overline{P_{\mathrm{s}}}$	Average supplied power to SS	W

we assume that the power consumption of the SS is equal to the supplied power to the SS, i.e., $\overline{P_{\mathrm{c}}} = \overline{P_{\mathrm{s}}}$. Hence, using (12) and (13), P_{req} is written as

$$P_{\mathrm{req}} = \frac{DP_{\mathrm{com}} + (1-D)P_{\mathrm{sleep}}}{1-D}. \tag{14}$$

Using (11) and (14), we eliminate P_{req} and solve for R_{max}, and then R_{max} is written as

$$R_{\mathrm{max}} = \frac{R_{\mathrm{lim}}c}{2f}\sqrt{\frac{\eta(1-D)G_{\mathrm{r}}S_{\mathrm{lim}}}{\pi[DP_{\mathrm{com}} + (1-D)P_{\mathrm{sleep}}]}}. \tag{15}$$

In addition, assuming $D \ll 1$, we approximate R_{max} as

$$R_{\mathrm{max}} \simeq \frac{R_{\mathrm{lim}}c}{2f}\sqrt{\frac{\eta G_{\mathrm{r}}S_{\mathrm{lim}}}{\pi(DP_{\mathrm{com}} + P_{\mathrm{sleep}})}}. \tag{16}$$

Using (15), we calculate R_{max} versus D. Table 9 shows the values of the parameters. In this analysis, there are two cases, i.e., frequency used for MPT is either 2.4 GHz or 900 MHz. Figure 10 shows the maximum distance R_{max} for each case. In Fig. 10, the horizontal axis indicates the duty ratio D. In addition, the vertical dashed line in Fig. 10 indicates the duty ratio in the experiment described in Sect. 5 ($D = 40\,\mathrm{ms}/10.24\,\mathrm{s} \approx 3.9 \times 10^{-1}\%$).

As shown in Fig. 10, the maximum distance realized by the system is longer using 900 MHz than using 2.4 GHz for MPT. In addition, even if the ES transmits microwave power using 2.4-GHz bands, the SS can receive sufficient power from the ES when $D \approx 3.9 \times 10^{-1}\%$, and the distance between the power transmitter and receive antennas is 10 m.

Table 9 Parameters for analysis.

Parameters	Values	
	Case 1	Case 2
f	2.4 GHz	900 MHz
R_{lim}	1 m	1 m
S_{lim}	10 W/m^2	6 W/m^2
G_{r}	7.7 dBi	7.7 dBi
η	95%	95%
P_{com}	100 mW	100 mW
P_{sleep}	1 μW	1 μW

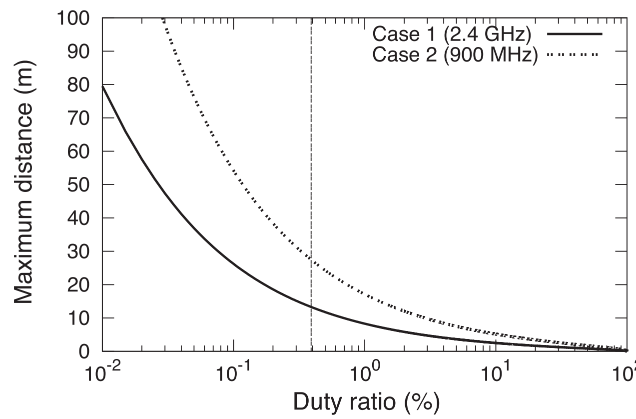

Fig. 10 Maximum distance realized by system.

7. Conclusion

In this paper, we have studied the implementation and feasibility of using MPT to operate an SS that communicates with ES on a WLAN, where the center frequency of the microwave frequency used for MPT is set to be the same as that of WLAN to achieve high spectral efficiency. To avoid the influence of MPT on WLAN data communications, the CSMA/CA protocol of WLAN could be a solution; however, throughput degradation due to data rate control and disassociation from the AP due to the association algorithm could happen.

In order to solve these problems and realize the largest possible coverage of MPT, we have proposed a scheduling scheme in which MPT and wireless communications operate in different periods of time, and the MPT supplies a maximal amount of energy to the SS. Thus, the SS needs to inform the ES of the timings of data frame transmissions. Recall that the purpose of this paper is to develop a scheduling scheme such that throughput degradation and disassociation problems due to the WLAN protocol are solved.

Then, we implemented the proposed scheduling system. From the results of experiments, we confirmed that the time sharing between MPT and WLAN data communications is successfully implemented. In addition, it is also confirmed that the remaining energy of the SS converges to the predetermined target value, i.e., the WLAN-based SS continuously works well.

Finally, on the basis of link budget analysis, we clarified the maximum allowable distance between the power transmitter and receiver antennas when the proposed scheduling scheme is utilized. As a result, we showed that the scheduling scheme can be applied to closed space or room.

Acknowledgment

This work was supported in part by JSPS KAKENHI Grant Number 24360149. This experiment was carried out using the Microwave Energy Transmission Laboratory (METLAB) system of the Research Institute for Sustainable Humanosphere at Kyoto University.

References

[1] F.L. Lewis, "Wireless sensor networks," in Smart environments: Technology, protocols and applications, pp.11–46, John Wiley & Sons, 2004.
[2] V. Shnayder, B. Chen, K. Lorincz, T.R.F. Jones, and M. Welsh, "Sensor networks for medical care," Harvard University Technical Report TR-08-05, vol.5, pp.314–314, April 2005.
[3] C. Yawut and S. Kilaso, "A wireless sensor network for weather and disaster alarm systems," Proc. International Conference on Information and Electronics Engineering, IPCSIT vol.6, 2011.
[4] N. Shinohara, "Power without wires," IEEE Microw. Mag., vol.12, no.7, pp.S64–S73, Dec. 2011.
[5] J. Hsu, S. Zahedi, A. Kansal, M. Srivastava, and V. Raghunathan, "Adaptive Duty Cycling for Energy Harvesting Systems," Proc. 2006 International Symposium on Low Power Electronics and Design (ISLPED'06), pp.180–185, Oct. 2006.
[6] A. Kansal, J. Hsu, S. Zahedi, and M.B. Srivastava, "Power Management in Energy Harvesting Sensor Networks," ACM Trans. Embedded Computing System, vol.6, no.4, Sept. 2007.
[7] T. Ichihara, T. Mitani, and N. Shinohara, "Study on intermittent microwave power transmission to a ZigBee device," Proc. IEEE IMWS-IWPT 2012, pp.209–212, Kyoto, Japan, May 2012.
[8] D. Maehara, R. Akai, G.K. Tran, K. Sakaguchi, S. Sampei, K. Araki, and H. Iwai, "Experiment on battery-less sensor activation via multipoint wireless energy transmission," Proc. IEEE PIMRC, pp.2336–2340, Sept. 2013.
[9] IEEE 802.11 Task Group ah (TGah) Sub 1 GHz license-exempt operation, http://www.ieee802.org/11/Reports/tgah_update.htm
[10] N. Imoto, S. Yamashita, T. Ichihara, K. Yamamoto, T. Nishio, M. Morikura, and N. Shinohara, "Experimental investigation of co-channel and adjacent channel operations of microwave power and IEEE 802.11g data transmissions," IEICE Trans. Commun., vol.E97-B, no.9, pp.1835–1842, Sept. 2014.
[11] "Radio-radiation protection guidelines for human exposure to electromagnetic fields," Telecommun. Technol. Council Ministry Posts Telecommun., Deliberation Rep.89, Tokyo, Japan, 1997.
[12] Arduino — ArduinoBoardFio, http://arduino.cc/en/Main/ArduinoBoardFio
[13] XBee Wi-Fi - Digi International http://www.digi.com/products/wireless-wired-embedded-solutions/zigbee-rf-modules/point-multipoint-rfmodules/xbee-wi-fi

Shota Yamashita received the B.E. degree in electrical and electronic engineering from Kyoto University in 2013. He is currently studying toward his M.E. degree at the Graduate School of Informatics, Kyoto University. His research interests include microwave power transmission for WLAN devices. He is a student member of the IEEE.

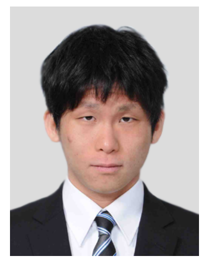

Norikatsu Imoto received the B.E. degree in electrical and electronic engineering from Kyoto University in 2012. He is currently studying toward his M.E. degree at the Graduate School of Informatics, Kyoto University. His research interests include microwave power transmission for WLAN devices. He is a student member of the IEEE.

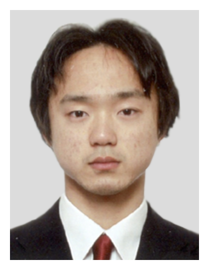

Takuya Ichihara received the B.E. degree in electrical and electronic engineering from Kyoto University, Japan in 2012. From 2012, he has been a student in the master course of electrical engineering in Kyoto University. He has been engaged in study on an Intermittent Microwave Power Transmission system.

Koji Yamamoto received the B.E. degree in electrical and electronic engineering from Kyoto University in 2002, and the M.E. and Ph.D. degrees in informatics from Kyoto University in 2004 and 2005, respectively. From 2004 to 2005, he was a research fellow of the Japan Society for the Promotion of Science (JSPS). Since 2005, he has been with the Graduate School of Informatics, Kyoto University, where he is currently an associate professor. From 2008 to 2009, he was a visiting researcher at Wireless@KTH, Royal Institute of Technology (KTH) in Sweden. His research interests include the application of game theory, spectrum sharing, and M2M networks. He received the PIMRC 2004 Best Student Paper Award in 2004, the Ericsson Young Scientist Award in 2006, and the Young Researcher's Award from the IEICE of Japan in 2008. He is a member of the IEEE.

Takayuki Nishio received the B.E. degree in Electrical and Electronic Engineering from Kyoto University in 2010, and the M.I. and Ph.D. degree in Communications and Computer Engineering, Graduate School of Informatics from Kyoto University, Kyoto, Japan, in 2012 and 2013 respectively. In 2013, he joined the faculty of Communications and Computer Engineering, Graduate School of Informatics, Kyoto University, Japan, where he is currently an Assistant Professor. His current research interests include network design, network management, and wireless communications particularly MAC and TCP design.

Masahiro Morikura received his B.E., M.E., and Ph.D. degrees in electronics engineering from Kyoto University, Kyoto, Japan in 1979, 1981 and 1991, respectively. He joined NTT in 1981, where he was engaged in the research and development of TDMA equipment for satellite communications. From 1988 to 1989, he was with the Communications Research Centre, Canada, as a guest scientist. From 1997 to 2002, he was active in the standardization of the IEEE 802.11a based wireless LAN. His current research interests include WLANs and M2M wireless systems. He received the Paper Award and the Achievement Award from IEICE in 2000 and 2006, respectively. He also received the Education, Culture, Sports, Science and Technology Minister Award in 2007 and Maejima Award in 2008. Dr. Morikura is now a professor in the Graduate School of Informatics, Kyoto University. He is a member of the IEEE.

Naoki Shinohara received the B.E. degree in electronic engineering, the M.E. and Ph.D. (Eng.) degrees in electrical engineering from Kyoto University, Japan, in 1991, 1993 and 1996, respectively. He was a research associate in the Radio Atmospheric Science Center, Kyoto University from 1998. He was a research associate of the Radio Science Center for Space and Atmosphere, Kyoto University by recognizing the Radio Atmospheric Science Center from 2000, and there he was an associate professor since 2001. He was an associate professor in Research Institute for Sustainable Humanosphere, Kyoto University by recognizing the Radio Science Center for Space and Atmosphere since 2004. From 2010, he has been a professor in Research Institute for Sustainable Humanosphere, Kyoto University. He has been engaged in research on Solar Power Station/Satellite and Microwave Power Transmission system. He is a member of the IEEE, URSI, the Institute of Electronics, Information and Communication Engineers (IEICE) and the Institute of Electrical Engineers of Japan (IEEJ).